Ninth International Conference on
THIN-WALLED STRUCTURES – ICTWS2023
Sydney, Australia, Nov 29 – Dec 1, 2023

PLASTIC MECHANISM MODELS FOR USE IN DSM LOCALISED LOADING DESIGN OF HAT SECTIONS UNDER ONE-FLANGE-LOADING

Zhehang Chen*, Cao Hung Pham and Gregory J. Hancock*****

* Doctoral Candidate, School of Civil Engineering, The University of Sydney, NSW 2006, Australia
e-mail: zhehang.chen@sydney.edu.au

** Associate Professor, School of Civil Engineering, The University of Sydney, NSW 2006, Australia
e-mail: caohung.pham@sydney.edu.au

** Emeritus Professor and Professorial Research Fellow, School of Civil Engineering,
The University of Sydney, NSW 2006, Australia
e-mail: gregory.hancock@sydney.edu.au

Keywords: Direct Strength Method, Steel Structures, Web-Crippling, Localised Loading.

Abstract. *The Direct Strength Method (DSM) of design has been recently developed for the design of cold-formed steel members under localised loading. The method requires a yield load (P_y) and an elastic buckling load (P_{cr}) as input variables to the DSM design equations. A recent paper by the authors at the CFSRC 2022 has summarised the development of plastic mechanism models based on experimental data to calculate P_y for hat sections with two flange loading cases. This paper summarises test results used to develop plastic mechanism models for calculating P_y for hat sections subject to one flange loading cases. Both Interior One Flange (IOF) and End One Flange (EOF) loading cases were investigated. The yield/plastic mechanism behaviour of multiple web sections is not yet fully understood, while several publications in the literature have discussed the mechanical behaviour of hat sections under localised loading. Hence, this paper attempts to explain and propose a plastic mechanism model for calculating the yield load (P_y) to be used in the DSM for localised loading design of hat sections in conjunction with the elastic buckling load P_{cr}, which is also described separately in this paper.*

1 INTRODUCTION

The research history of the web crippling phenomenon in cold-formed steel structural members dates back to the early 1940s. Due to the complexity of theoretical and analytical analyses, most of the formulae were developed on the basis of empirical data and a curve fitting method. Bakker and Peköz [1] have pointed out the fact that while most of the curve-fitting formulae fit the test results on which they are based, they show poor correlation with other formulae derived from similar research. In recent years, this problem has been partially solved by a newly developed design method namely the Direct Strength Method, which has been well developed and incorporated in the North American Specification AISI S100 [2] and the Australian/New Zealand Standard AS/NZS 4600 [3] for design of cold-formed steel sections under compression by Schafer [4][5], bending by Schafer and Peköz [6], and shear by Pham and Hancock [7]. As of today, there have been no DSM design rules for cold-formed structural members subjected to localised loading in this specification and standard.

Recently, a paper published by Chen, Pham, Hancock [8] has shown that the DSM can be used for the design of hat sections under localised loading. A simplified and consistent yield load model for P_y based on a plastic mechanism was proposed for use in DSM localised loading design of hat sections under Two Flange (TF) loading. A new form of DSM equations, which was developed and published by Glauz and Schafer [9], was used in [8]. Factors for the ITF

and ETF loading cases for use in the new DSM equations were proposed in [8] using the laboratory tests.

A second series of laboratory tests on the One Flange (OF) loading cases with various fastening conditions has been recently conducted and is summarised in this paper. Plastic mechanism models for calculating the P_y for the Interior One Flange (ITF) and End One Flange (EOF) cases are proposed and explained. In addition to the variables investigated in the TF loading cases, the fastening condition is also considered as an important variable in the EOF loading case. The experimental data is compared with the proposed DSM design equations for the different loading cases.

2 YIELD LOAD

2.1 Basic concept of DSM

Generally, the DSM design equations are based on two input variables: an elastic buckling load (P_{cr}) and a yield load (P_y). The methods for calculating the buckling load are well established and described in another paper at this conference by Hancock et al. [10]. It provides a review of different methods for calculating buckling loads currently, which are available for localised loading buckling analyses. Two of the introduced methods namely the Finite Element Method (FEM) and the Finite Strip Method (FSM) are compared numerically in [10].

Hofmeyer [7,8] proposed a series of complex equations for calculating the exact plastic hinge locations for hat section under localised loading in the IOF loading conditions. However, it was not considered as a proper method for calculating the yield load for DSM design equations for the following reasons: (i) that set of equations requires complex calculations including but not limited to multiple iterations, (ii) it can only be used for calculating a strip of hat section which makes it difficult to perform manually, (iii) it was only limited to the IOF loading case without considering the slope of the web and the fastening condition of the bottom flange.

In this paper, the simplified generic model for calculating the yield load, which is generally derived from plastic mechanism model and was proposed in [8] for the TF loading cases, is adopted and modified for use in the OF loading cases.

2.2 General plastic mechanism model for vertical web sections

A general plastic mechanism model has been proposed based on the yielding behaviour observed from experiments and various FEM simulation models developed by the authors. Fig. 1 demonstrates the general plastic mechanism model for hat sections subjected to localised loading for the ITF-F and ETF-F loading cases where the "-F" refers to the fastening condition. For hat sections, the bottom flanges are always fastened to the bearing plate.

The proposed yield load P_y is given by

$$P_y = k_w F_{sw} \tag{1}$$

where

k_w is the number of webs in the section. For Hat sections, k_w = 2;

F_{SW} is the load calculated for a single web.

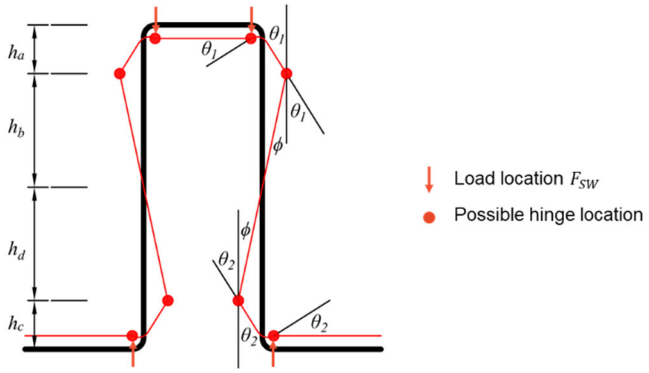

Figure 1 General plastic mechanism model for hat sections subject to localised loading, for the ITF-F and ETF-F loading cases

The general equation for the capacity of a single web of a hat section under localised loading was derived using the virtual work principle in Chen et al. [8] and is given by

$$F_{SW} = \frac{M_p}{k_\theta r_c} \times \sum_{i=1}^{n} k_{\omega_i} L_i \tag{2}$$

$$M_p = \frac{f_y t^2}{4} \tag{3}$$

where

k_θ is a factor for the number of loaded flanges. For two-flange loading cases (ITF, ETF), $k_\theta = 2$ and for one-flange loading cases (IOF, EOF), $k_\theta = 1$;

k_{ω_i} is a factor for the rotation angle at each plastic hinge;

r_c is the centreline corner radius. $r_c = r_{in} + 0.5t = r_{ext} - 0.5t$, where r_{in} is the inside corner radius, r_{ext} is the external corner radius and t is the thickness of the section;

M_p is the plastic moment per unit length of plate.

It should be noted that for the One Flange (OF) loading cases, depending on the loading conditions, some of the yield lines in the generic model might no longer exist, resulting in some of the values in the generic model no longer being used. Based on the observation from the FE model, assumptions are made specifically for each of the OF loading cases for simplification.

For the OF loading cases, since the hat section is loaded from either the top flange or the bottom flanges, the yield lines are only formed near the loaded flanges as follows.

In the IOF loading case where the load is on the top flange,

$$h_a + h_b = H, h_c = h_d = 0, \theta_2 = 0 \tag{4}$$

In EOF loading case where the load is on the lips, regardless of the fastening condition,

$$h_c + h_d = H, h_a = h_b = 0, \theta_1 = 0 \tag{5}$$

In Equations (4) and (5), the k_{ω_i} value can be calculated.

Based on these simplifications and observations, the plastic mechanism models for the OF loading cases are redrawn as Figs. 2(a) and 2(b). According to the availability of the yield lines, Equation (3) can be rewritten for each of the OF loading cases.

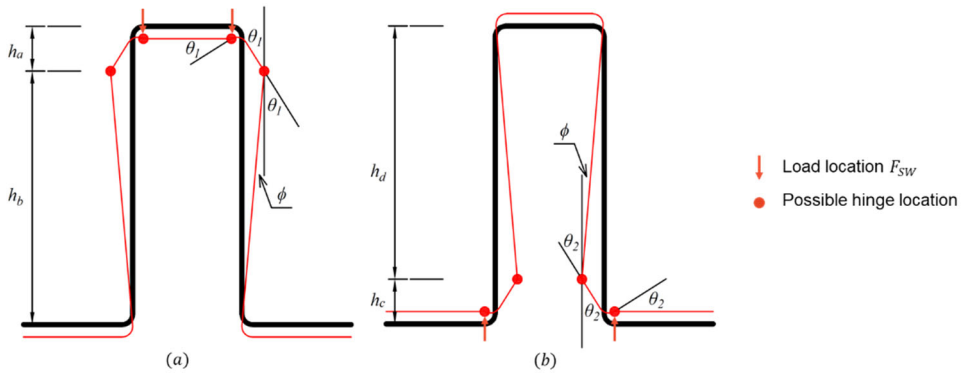

Figure 2 Plastic mechanism model for hat sections subject to localised loading, for IOF(a) and EOF(b) loading cases

2.3 Length of yield line

Similar to the Two Flange (TF) loading cases, the methodology for predicting yield line length is similar to the method proposed for tubular sections by Zhao and Hancock [13], which has been included in the Australian Standard AS4100 [14]. Using Figs. 2 and 3 to guide the fastened cases, two yield lines need to be included in the yield load calculation, while only one yield line in the web needs to be considered for unfastened cases.

By taking the IOF-F loading case as an example, the lengths of the yield line on the top of flange (L_{TF}) and top of the web (L_{TW}) are calculated as follows.

$$L_{TF} = L_w + 2t \tag{6}$$

$$L_{CT} = L_{TF} + 2 \times k_{dc} \times r_c \tag{7}$$

$$L_{TW} = L_{CT} + 2 \times k_{dw} \times (a - r_c) \tag{8}$$

where

L_w is the bearing length of the bearing plate.

L_{CT} is the length at the intersection between the top corner and the web.

$k_{dc} = 1/\tan\gamma_1$ where γ_1 is the diffusion angle in the corner as shown in Fig. 3.

$k_{dw} = 1/\tan\gamma_2$ where γ_2 is the diffusion angle in the web as shown in Fig. 3.

k_{dc} and k_{dw} are given in Table 1.

Table 1: Summary of the exponents and factors for the Py model

(F=Fastened, UF=Unfastened, Y=yield line exists, N= yield line does not exist)

Load Case	Fastening Condition	k_θ	k_H	k_{dc}	k_{dw}	L_{TF}	L_T	L_B	L_{BF}
ITF	F	2	0.25	2.5	2	Y	Y	Y	Y
ETF	F	2	0.25	2.5	2	N	Y	Y	N
IOF	F	1	0.33	2.5	2	N	Y	N	N
EOF	F	1	0.33	2.5	1	N	N	Y	Y
EOF	UF	1	0.33	2.5	2	N	N	Y	N

k_H is equal to h_a/H or h_c/H depending on the loading case.

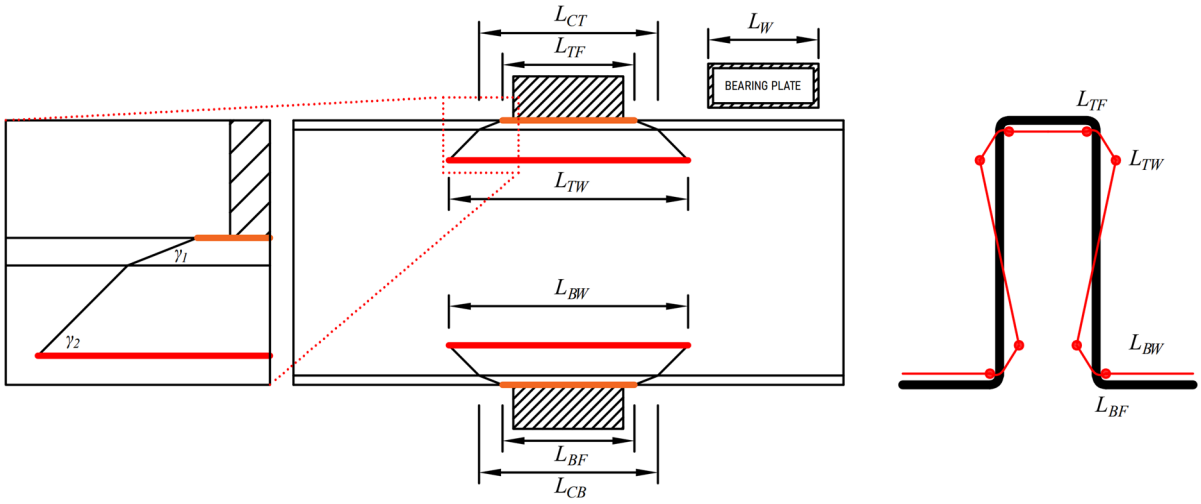

Figure 3 Side view of general plastic mechanism model and detail of the slope

2.4 Summary of the exponent and factors for the P_y model

The factors of the P_y models are based on the initial yield line locations before significant position shifting, also known as first yield location in accordance with observation from the verified FE analysis. A summary of the exponents and factors for the P_y model of the hat sections for both the TF and OF loading cases is given in Table 1.

2.5 Adjustments and amendments

The reduction in the plastic moment capacity for axial compression was developed by Zhao and Hancock [13] as used in Chen et al. [8] as given by Equation (9). For the OF loading cases, adjustment regarding plastic moment capacity and amendments for sloped web sections remains the same as that in the TF loading cases.

$$M_p' = \frac{f_y t^2 L_s}{4}\left[1 - \left(\frac{P}{f_y L_s t}\right)^2\right] \tag{9}$$

where

L_s is the length of the yield line.

f_y is the yield stress of the material.

It should be noted that an iterative method is required since P is a function of the value of P_y being calculated. Normally two iterations are sufficient.

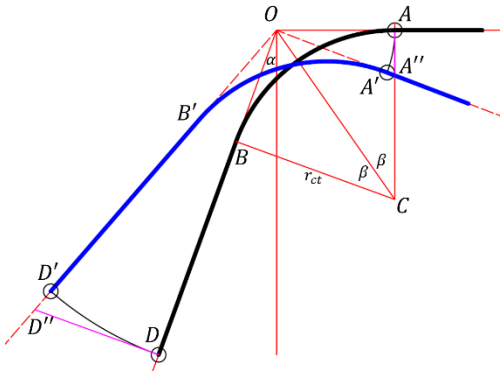

Figure 4 Corner details of sloped web sections

For the sloped web sections, a factor $1/\tan\beta$ is introduced into Equation (2) to consider the change of eccentricity where β is half of the angle α for the slope of the web as shown in Fig. 4. Thus, Equation (2) can be rewritten as Equation (10).

$$F_{SW} = \frac{1}{\tan\beta} \times \frac{M_p}{k_\theta r_c} \times \sum_{i=1}^{n} k_{\omega_i} L_i \tag{10}$$

3 EXPERIMENTAL RESEARCH DATA

A set of tests on hat sections under localised loading cases have been found in previous research. The only detailed tests have been conducted by Wu et al. [15] and are limited to slender hat sections with sloped webs. Also, as per Wu's tests, only the IOF-F and EOF-UF loading cases were tested for the OF cases. As a result, it was found that systematic testing on stocky hat sections, similar to the TF loading cases, is needed. In this chapter, the experimental setup for the OF loading cases are discussed.

3.1 Stocky section tested by Chen, Pham and Hancock

Similar to the first series of web crippling tests designed and conducted by the authors on the TF cases as reported in [8], stocky sections with the same thickness and dimensions were used for consistency in the second series as reported in this paper. The "Test Standard for Determining the Web Crippling Strength of Cold-Formed Steel Flexural Members", which is also known as AISI S909 [16], was selected as the guideline for designing and performing the whole series of tests.

Unlike the TF loading cases, where the flanges at the bottom were fully fastened to the bearing plate, three different OF loading cases were tested. For the IOF loading cases, the bottom flanges of the specimen were fastened to the bearing plate at both ends in line with most practical use conditions. The bottom flanges under the mid-span of the specimen were also tied by a strip to prevent significant shape distortion as guided by the test standard.

On the other hand, specimens with both fastened and unfastened cases were tested for the EOF loading cases. For the EOF-F loading case, both vertical and sloped web sections were tested, while for the EOF-UF loading case, only vertical web sections were tested. The reason for performing vertical web sections only is that the cross-section shapes of sloped web sections are likely to change due to a splaying effect. This was not the case for Wu's test because the sections are thin enough to reach the buckling load before the bottom flange starts to slip. Fig. 5 demonstrates the setup for the OF loading cases subjected to IOF and EOF loading cases, respectively. In order to prevent the localised failure modes at unwanted loading/support zones, stiffening blocks such as those shown in yellow in Fig. 5(a) and stiffening plates such as those at the centre of the section in Fig. 5(b) were used during the tests at designated positions.

The dimensions of the specimen were carefully designed to be identical to those in the previous series of experimental testing in the TF loading cases so that comparable results could be obtained between the loading cases and the OF loading cases. Fig. 6 shows dimensions and nomenclature of a typical hat section. It should be noted that for the OF loading cases, LB is recorded as the loading-related dimension. For example, for the IOF loading cases, the relevant dimension of LB is defined as the bearing width in the middle as shown in Fig. 6.

All the test data dimensions including the corner radii and the final maximum loads are given in Table 2. It should be noted that the width of top flange W as shown in Fig. 6 is 150 mm for all sections. The width of bottom flanges, the width of return lips and the internal corner radius between bottom flanges and return lips are 35 mm, 15 mm and 6 mm respectively for all sections.

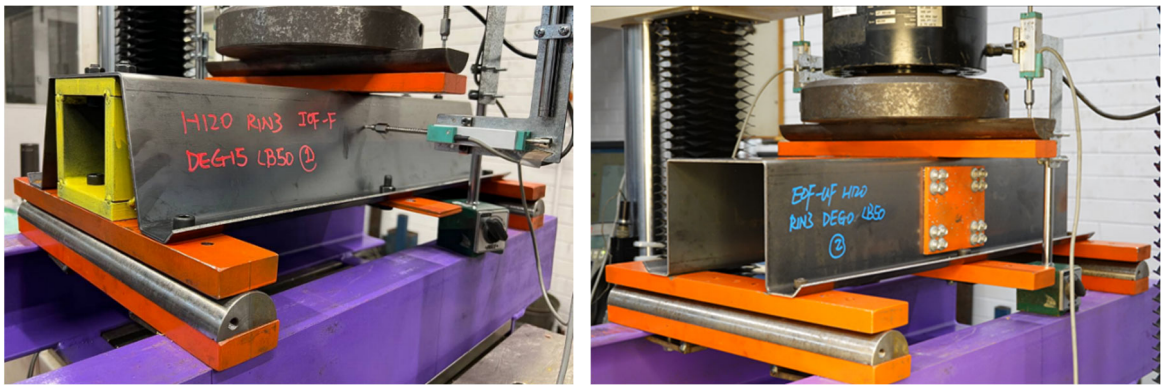

(a) (b)

Figure 5 setup of a typical web crippling test, IOF loading case (a) and EOF loading case (b)

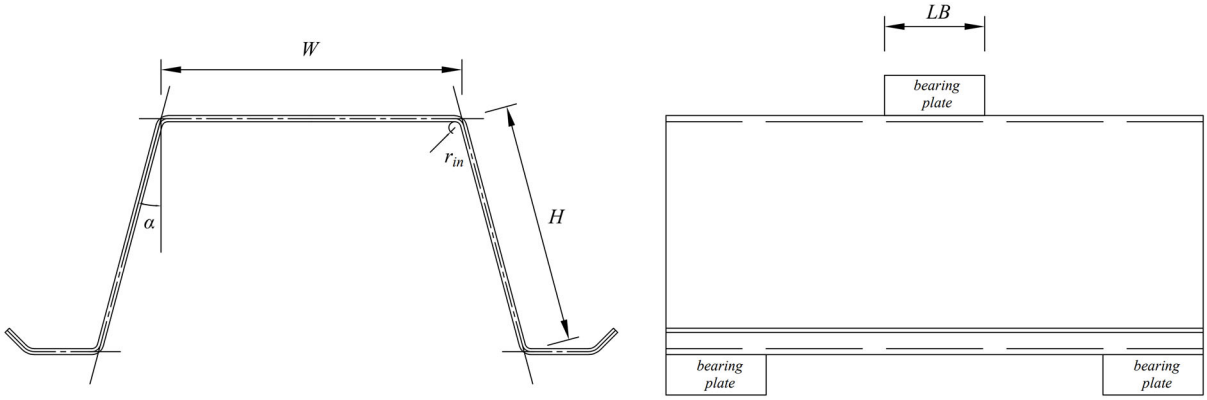

Figure 6 Dimension definition of hat sections, for OF loading cases

Table 2: Test results for IOF and EOF loading cases.

Tests	P_{max_1} (kN)	P_{max_2} (kN)	P_{max_3} (kN)
IOF-F-H120-RIN3-DEG0-LB100	80.205	80.425	
IOF-F-H120-RIN3-DEG0-LB50	-	62.608	63.761
IOF-F-H120-RIN3-DEG15-LB50	61.802	60.886	
IOF-F-H120-RIN3-DEG30-LB50	61.491	61.619	
IOF-F-H120-RIN8-DEG0-LB100	64.567	63.578	
IOF-F-H120-RIN8-DEG0-LB50	50.082	50.339	
IOF-F-H120-RIN8-DEG15-LB50	50.815	50.870	
IOF-F-H120-RIN8-DEG30-LB50	49.167	49.368	
IOF-F-H90-RIN3-DEG0-LB50	59.330	58.286	
IOF-F-H90-RIN8-DEG0-LB50	46.365	45.816	
EOF-F-H120-RIN3-DEG0-LB50	87.218	94.250	
EOF-F-H120-RIN3-DEG15-LB50	93.408	91.064	
EOF-F-H120-RIN3-DEG30-LB50	92.529	94.177	93.847
EOF-F-H120-RIN8-DEG0-LB50	68.760	71.104	
EOF-F-H120-RIN8-DEG15-LB50	71.104	71.800	
EOF-F-H120-RIN8-DEG30-LB50	71.818	72.533	72.514
EOF-F-H90-RIN3-DEG0-LB50	97.693	98.828	96.264
EOF-F-H90-RIN8-DEG0-LB50	73.430	75.316	73.448
EOF-UF-H120-RIN3-DEG0-LB50	78.630	82.842	81.377
EOF-UF-H120-RIN8-DEG0-LB50	60.154	59.018	

Similar to the TF tests, for the OF loading cases, small deformation is expected to occur and controlled loading displacement is set to 10 mm minimum (or equivalent to a minimum of 8.3%

of the length of the web) unless a significant drop in the load – displacement curve was observed within 10 mm displacement. During the test, the load from the load cell P and the displacement of the load cell Δ were recorded. The loading capacity P_{exp} is defined as the maximum load capacity within an acceptable range of deformation during the test. In this case, it is recorded as the maximum load P_{max} recorded in the first 10 mm displacement. It is worth mentioning that the serviceability limit of deformation does not apply here because the purpose of this test is mainly about the strength not the serviceability.

For the OF loading cases, it was found that the failure modes as proposed by Bakker and Stark [17] can be extended to the OF loading cases, at least valid for the initial loading stage. For a later stage, a yield arc post-failure mode can be observed in most cases regardless of the initial failure mode. However, the difference between small and large corner radii sections in the load – deflection curves is still visually distinguishable, where a gradually increasing trend for large corner radius sections compared to a sharp increasing trend in small radius sections with a defined maximum can be identified.

3.2 Slender section tested by Wu, Yu and LaBoube

A series of web crippling tests for hat and decking sections using Grade 80 of A653 steel were conducted by Wu, Yu and LaBoube [15]. Only tests on the IOF-F and EOF-UF loading cases were performed. For each loading case, six of those tested specimens were found to be similar to the tests in this paper and can be used as reference data in the slender range of the DSM curve. The dimensions and test results from the research report are collected and given in Table 3.

It should be noted that Wu et al. [15] did not report any information on the EOF-F loading case. Consequently, some additional data has been generated using an FEM analysis to allow a full DSM curve to be defined and calibrated for the EOF-F case. The FEM analysis is described separately in Chen [18], and the results for the EOF-F case are summarised in Table 4.

Table 3: Dimensions and test results collection from Wu's test, IOF-F and EOF-UF loading cases

Load Case	Fastening Condition	H (mm)	RIN (mm)	DEG (degree)	LB (mm)	P_{max} (kN)
IOF	F	76.2	1.9844	30	38.1	8.015
IOF	F	76.2	1.5875	30	38.1	8.195
IOF	F	114.3	1.9844	30	38.1	7.324
IOF	F	114.3	1.5875	30	38.1	7.533
IOF	F	152.4	1.9844	30	38.1	6.823
IOF	F	152.4	1.5875	30	38.1	7.406
EOF	UF	76.2	1.9844	30	25.4	3.841
EOF	UF	76.2	1.5875	30	25.4	4.128
EOF	UF	114.3	1.9844	30	25.4	2.994
EOF	UF	114.3	1.5875	30	25.4	3.274
EOF	UF	152.4	1.9844	30	25.4	2.462
EOF	UF	152.4	1.5875	30	25.4	2.671

Table 4: Dimensions and simulation results from ABAQUS using Wu's sections, EOF-F loading case

Load Case	Fastening Condition	H (mm)	RIN (mm)	DEG (degree)	LB (mm)	P_{max} (kN)
EOF	F	76.2	1.9844	30	25.4	4.221
EOF	F	76.2	1.5875	30	25.4	4.397
EOF	F	114.3	1.9844	30	25.4	3.212
EOF	F	114.3	1.5875	30	25.4	3.277
EOF	F	152.4	1.9844	30	25.4	2.599
EOF	F	152.4	1.5875	30	25.4	2.607

4 THE DSM EQUATION

4.1 General formulae for DSM equation

In order to be consistent with the new form of DSM equations developed and published by Glauz and Schafer [9] and also used in [8], the general formulae for the DSM equations is given as:

$$\frac{P_n}{P_y} = k_p \frac{1+a\lambda^c}{1+b\lambda^d} \tag{11}$$

where

P_n is the nominal load capacity for localised loading;

P_y is the yield load;

λ is the slenderness, calculated using following equation:

$$\lambda = \sqrt{P_y/P_{cr}} \tag{12}$$

4.2 Explanation for the factors used in the DSM equations

By definition, it is not hard to understand that the values of c and d should be taken as 2 because of the physical meaning of λ, which is a slenderness based on a square root.

As a prefix for the DSM equation, k_p is considered as a factor for scaling the DSM curve in the y axis (strength) direction. If no scaling is required, k_p should be taken as 1 by default. However, according to Glauz and Schafer [9], k_p is only taken as 1.2 for the DSM equations for shear to allow some post first yield reserve in shear. For bending, since the section bending capacity is taken as M_p, then k_p is taken as 1.0, and for compression since P_y is true first yield, then k_p is also taken as 1.0.

While there is no specific meaning for the factors a and b, it is found that the value a/b is of importance for the DSM design curve. Assuming $k_p = 1, c = d = 2$, we have:

$$\lim_{\lambda\to 0} \frac{P_n}{P_y} = 1\,,\ \lim_{\lambda\to \infty} \frac{P_n}{P_y} = \frac{a}{b} \tag{13}$$

which indicates that the DSM curve P_y/P_n is a curve that starts from 1 and asymptotes to a/b when λ is large. When "a/b" is constant, a smaller value of "a" results in a slower reduction in P_y/P_n. A different "a/b" value can be found in each of the DSM equations for the different loading conditions published by Glauz and Schafer [9] as well as in Chen et al. [8].

4.3 Calculation step of P_n

The calculation of P_n can be separated into three parts.

(1) P_y is calculated by the proposed plastic mechanism model without iteration followed by two iteration calculations as described in [8]. The calculated P_y after two iterations, noted as $P_y^{''}$ is used for further calculation as an amended P_y.

(2) P_{cr} is calculated by either FEM (ABAQUS) or FSM (THIN-WALL). Once λ is calculated, P_n/P_y can be determined by the relevant DSM design equation.

(3) P_n can be calculated by using the amended P_y times P_n/P_y.

A flow chart for the determination of P_y is illustrated in Fig. 7.

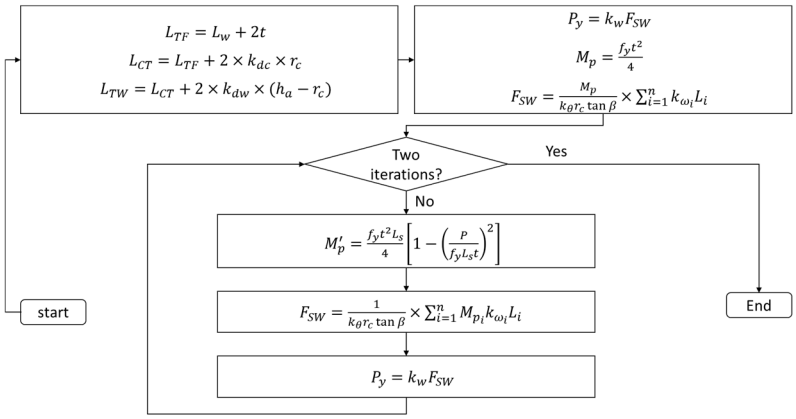

Figure 7 A flow chart for calculation of Py

5 VERIFICATION AND DISCUSSION

For the IOF and EOF loading cases, the factors computed from the tests and used in the DSM equations are given in Table 5 as compared with the values for the TF loading cases in [8].

Table 5: Summary of the exponents and factors for Chen's DSM equations

Load Case	Fastening condition	a/b	a	b	c	d	k_p
ITF	F	0.0933	0.14	1.5	2	2	1
ETF	F	0.0357	0.05	1.4	2	2	1
IOF	F	0.0933	0.14	1.5	2	2	1
EOF	F	0.0947	0.18	1.9	2	2	1
EOF	UF	0.0750	0.12	1.6	2	2	1

The predicted load capacities and the test results are compared for IOF-F, EOF-F and EOF-UF loading cases in Figs. 8, 9(a) and 9(b). Results using different internal corner radii (3 mm and 8 mm) are plotted in different colours.

For all the OF loading cases, the data for smaller 3 mm corner radius sections show good alignment with the DSM design curve predictions. The predictions for larger corner radius sections with the DSM curves show a conservative result. The reason for the conservative prediction in the large corner radius sections is due to the difference in failure modes. Unlike the TF loading cases, in both the smaller and larger corner radii sections, a peak value can be observed on the load – displacement curve. Since yield-arc and rolling failure modes, which were first described by Bakker and Stark [17], still occurred in the early yielding stage, a different yielding process is observed between the smaller and larger corner radii sections so that reaching the plateau requires more controlled vertical displacement for larger corner radius sections.

Further, as the concept of the DSM aims to provide a consistent and simplified model for both the small and large corner radii sections, it is difficult and impractical to use a simple mechanism model to pick up all the different mechanical behaviours. Thus, the P_y calculation does not cover the precise prediction of the contribution from the rolling behaviour. A conservative result is therefore selected to cover greater uncertainties.

It should be noted that the chosen DSM design curves also fit the slender section test data from Wu, Yu and LaBoube [15] in the IOF-F and EOF-UF loading cases, respectively. For the EOF-F loading case, the results from the FE simulations (ABAQUS), using the cross sections from Wu's tests, provide strong support for the adequacy of the DSM design equation.

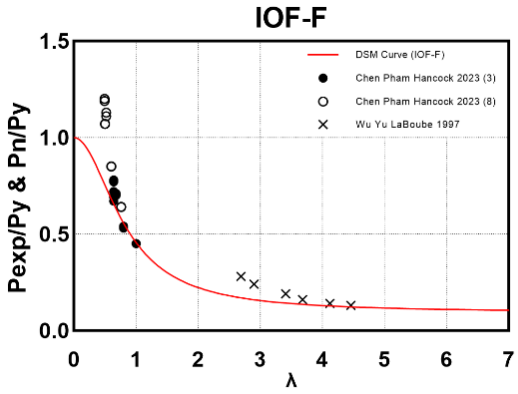

Figure 8 DSM curve for hat sections, IOF fastened

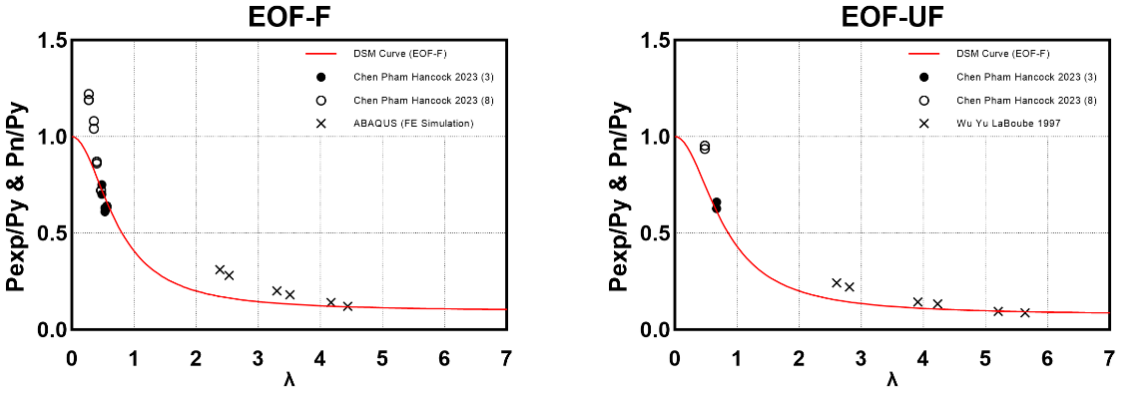

(a) (b)

Figure 9 DSM curve for hat sections, EOF fastened (a) and unfastened (b)

6 CONCLUSION AND FUTURE RESEARCH

6.1 Conclusion

This research provides strong evidence that the Direct Strength Method (DSM) can be used for the design of hat sections under localised loading in the One Flange (OF) loading cases. Together with the previous research study specifically for the TF loading cases also performed by the authors, a DSM equation has been proposed along with a set of factors to cover most of the practical loading cases.

The simplified and consistent P_y model based on a plastic mechanism has been extended to cover both the TF and OF loading cases for use in the DSM localised loading design of hat sections.

With respect to the test results, most of the practical loading cases recommended by the testing specification have been tested using stocky sections for better understanding the yielding and plastic mechanism behaviour. The proposed DSM design equations also extend the type of hat sections to those with sloped webs and including the reduction in the plastic moment capacity for axial compression.

6.2 Future research

A hypothesis is made regarding the a/b in the general DSM equation where a/b is a factor can apply to different practical loading scenarios. The a/b value should stay within a specific number for the same loading scenario. Given that there is no available experimental data

regarding slender sections using the same or similar dimension, the application of the DSM, especially in the slender range, is still in the provisional stage. Extra test data is required for the calibration of the DSM design equations at higher slenderness as may occur in practice.

It should be noted that the curve asymptotes to a/b at high slenderness in the new form of the DSM equation. This is behaviourally incorrect because it should keep reducing in association with slenderness. Given that the slenderness cannot be too large, an upper limit on the slenderness might be required. In order to determine the upper slenderness, further research, specifically on slender sections, is necessary.

REFERENCES

[1] M. Bakker, T. Peköz, Comparison and evaluation of web crippling prediction formulas, *Cent. Cold-Formed Steel Struct. Libr*. (1985). https://scholarsmine.mst.edu/ccfss-library/152.

[2] AISI, *North American Specification for the Design of Cold-Formed Steel Structural Members NAS S100-2016*. American Iron and Steel Institute, Washington, DC.

[3] Standards Australia, AS/NZS 4600:2018: *Cold-formed steel structures*, 2005 (2018).

[4] Schafer B.W., "Distortional buckling of cold-formed steel columns", Final Report, Sponsored by the American Iron and Steel Institute, Washington, DC, 2000.

[5] Schafer B.W., "Local, distortional and Euler buckling in thin-walled columns", *Journal of Structural Engineering*, ASCE, 64 (7/8), pp 766-778, 2008.

[6] Schafer B.W. and Pekoz T., "Direct Strength Prediction of cold-formed steel members using numerical elastic buckling solutions", *Fourteenth International Specialty Conference on Cold-Formed Steel Structures*. St. Louis, Missouri, USA. 1998.

[7] Pham, C.H. and Hancock, G.J., "Direct strength design of cold-formed C-sections for shear and combined actions", *Journal of Structural Engineering, ASCE*, 138 (6), 2012.

[8] Z. Chen, C.H. Pham, G.J. Hancock, Yield Models for use in DSM Localised Loading Design of Hat Sections, 2022 (2022) 1–13. https://jscholarship.library.jhu.edu/handle/1774.2/40427.

[9] R.S. Glauz, B.W. Schafer, Modifications to the Direct Strength Method of cold-formed steel design for members unsymmetric about the axis of bending, *Thin-walled Structures*, 173 (2022) 109025

[10] G.J. Hancock, Z. Chen, Y. Xie, C.H. Pham, Recent developments in the DSM localised loading design of cold-formed steel sections, Ninth Int. Conf. *Thin-walled Structures*, Sydney. (2023).

[11] H. Hofmeyer, Cross-section crushing behaviour of hat-sections (Part I: Numerical modelling), *Thin-walled Structures*, 43 (2005) 1143–1154. https://doi.org/10.1016/j.tws.2005.03.009.

[12] H. Hofmeyer, Cross-section crushing behaviour of hat-sections (part II: Analytical modelling), *Thin-walled Structures*, 43 (2005) 1155–1165. https://doi.org/10.1016/j.tws.2005.03.012.

[13] X.L. Zhao, G.J. Hancock, Experimental verification of the theory of plastic-moment capacity of an inclined yield line under axial force, *Thin-walled Structures*, 15 (1993) 209–233.

[14] Standards Australia, AS 4100-1998 (R2016): *Steel structures*, 1998 (2016).

[15] S. Wu, W. Yu, R.A. Laboube, Strength of flexural members using structural grade 80 of A653 steel (web crippling tests), (1997).

[16] AISI S909-(2017), Test Standard for Determining the Web Crippling Strength of Cold-Formed Steel Flexural Members, (2017) 15–25.

[17] M.C.M. Bakker, J.W.B. Stark, Theoretical and experimental research on web crippling of cold-formed flexural steel members, *Thin-walled Structures*. 18 (1994) 261–290.

[18] Z. Chen, Direct Strength Method for the Design of Cold-formed Steel Hat Sections under Localized Loading (in preparation), PhD Thesis. (2023).